

Supporting Information

Constructing Highly Selective Multidirectional Hydrogel Strain Sensors with Pre-stretching Strategy

*Wenqi She, Chong Shen, Zaifei Xue, Jie Yu, Guoliang Zhang and Qin Meng**

Material and Methods:

Synthesis of F127-DA: In a three-neck flask, 26 g of Pluronic® F127 (PEO₉₉-PPO₆₅-PEO₉₉, Sigma-Aldrich, USA) was completely dissolved in 100 mL of tetrahydrofuran (THF, Sinopharm Chemical Reagent, China) under continuous stirring at 40 °C. Upon complete dissolution, triethylamine (3.84 mL, Sinopharm Chemical Reagent, China) and acryloyl chloride (3.52 mL, Aladdin, China) were gradually introduced dropwise under ice-water cooling. Following a 24-hour reaction under a nitrogen atmosphere at 30 °C, the byproduct triethylammonium chloride was separated via filtration, and the supernatant was subjected to precipitation by using anhydrous ether (Sinopharm Chemical Reagent, China). The crude product was subsequently dried under vacuum for 4 h. To enhance acrylate grafting, this process was repeated twice. The purified polymer was then redissolved in deionized water, dialyzed through a 7 kDa dialysis membrane (Solarbio, China) for 7 days, and freeze-dried to obtain purity F127-DA.

Hydrogel Fabrication: Solutions with different F127-DA contents (2 wt%, 3 wt%, 4 wt% and 5 wt%) were prepared by dissolving the polymer into 0.5 wt% CS (Sinopharm Chemical Reagent, China) solution containing glycerol under magnetic stirring. Unless otherwise specified, the mass ratio of glycerol to CS solution was maintained at 1:1. After full dissolution, 1 g of AM (Aladdin, China) and 0.025 g of Iragcure 2959 (Alfa Aesar, USA) were gradually added to 4 g of the above-prepared solution while stirring for 10 min to ensure homogeneity. To eliminate dissolved oxygen and minimize air bubble formation, nitrogen gas was purged through the mixture for 5 min under gentle shaking. The mixed solution was then irradiated with UV light (LIBI UV-400, China) for 1 min to form the PCFG hydrogel. In this case, the PCMG hydrogel was prepared by adding an equimolar amount of MBA, equal to 4 wt% F127-DA.

Characterization and Measurements of the hydrogel: The mechanical properties of the hydrogels were evaluated through tensile stress–strain and cyclic loading–unloading tests

using a Universal Testing Machine (QLW-5E, Qunlong, China). The samples were cut into dumbbell shapes ($50 \text{ mm (l)} \times 8.5 \text{ mm (d)} \times 2 \text{ mm (w)}$), and the stretching speed was 10 mm min^{-1} . The long-term stability of the hydrogels under ambient conditions was assessed by monitoring their weight retention over time. Hydrogels were placed in open-air environments at $25 \pm 2 \text{ }^\circ\text{C}$ with a relative humidity of $55 \pm 5\%$ to test the long-term stability. The weight of the Hydrogels was recorded at fixed time intervals, and the retained weight percentage was calculated based on the initial mass to evaluate water retention capacity. The crystallization/melting behavior of the hydrogels was measured using differential scanning calorimetry (DSC, TA 2500, USA). The prepared hydrogels were cooled from room temperature to $-80 \text{ }^\circ\text{C}$ at a rate of $5 \text{ }^\circ\text{C min}^{-1}$ and then heated to $30 \text{ }^\circ\text{C}$ at a rate of $5 \text{ }^\circ\text{C min}^{-1}$. The freezing point of the hydrogels was determined as the peak temperature observed during the heating cycle.

Synthesis of MXene: MXene was obtained using the LiF–HCl etching method. Briefly, 1 g of Ti_3AlC_2 MAX phase powder (Bknano, China) was slowly added to 20 mL of 9 M HCl (Sinopharm Chemical Reagent, China) and 1 g LiF (Aladdin, China) mixed solution. The mixture was stirred magnetically at $35 \text{ }^\circ\text{C}$ for 24 h in an Ar atmosphere and then washed multiple times through deionized water at 3500 rpm until the supernatant reached a pH ~ 6 . The supernatant was sonicated in an ice bath for 2 h, followed by centrifugation at 3500 rpm for 1 h to remove unexfoliated precursors. The exfoliated MXene nanosheets were extracted from the supernatant, yielding a stable colloidal dispersion with a final MXene concentration of approximately 20 mg mL^{-1} .

Fabrication of Hydrogel Sensor: The AgNW used in this study were commercially sourced from Shanghai Ouyi Organic Optoelectronic Materials Co., Ltd., with a diameter of 30–60 nm, a length of 10–20 μm , and a purity of 99% (metal basis). The PCFG-4 hydrogel substrate was initially dried using lint-free paper and subsequently air-blown with compressed gas for 30 s. Following high-speed centrifugation, the MXene solution ($\sim 30 \text{ mg mL}^{-1}$) was uniformly coated onto the biaxially pre-stretched hydrogel (100%) using the doctor blade technique and dried in a vacuum oven at $60 \text{ }^\circ\text{C}$ for 30 s. The hydrogel was then gradually released to its original dimensions before being uniaxially pre-stretched to 100% along the a-axis direction. The AgNW solution ($\sim 10 \text{ mg mL}^{-1}$) was sprayed onto the pre-stretched hydrogel surface using a precision spray gun and subsequently dried in a vacuum oven at $60 \text{ }^\circ\text{C}$ for 1 min. The hydrogel was then slowly released to its original state. For multidirectional strain sensor fabrication, two AM-PCFG-4 hydrogel sensors were assembled in an orthogonal

configuration. A thermoplastic polyurethane (TPU) film was inserted between the two AM-PCFG-4 hydrogel sensors as a spacer to prevent cross-interference between the active sensing films. Finally, copper wires were attached at the terminal ends along the y-axis direction of each individual AM-PCFG-4 sensor.

Characterization and Measurements of the hydrogel strain sensor: The chemical compositions of samples were tested by ATR-FTIR (Nicolet iS50, Thermo Fisher, USA) from 4000 to 400 cm^{-1} at a resolution of 4 cm^{-1} . The structural Evolution of the AM-PCFG-4 anisotropic hydrogel strain sensor was observed by a field emission scanning electron microscope (FE-SEM, Hitachi, SU-8010, Japan). The electromechanical performance of sensors was evaluated on a universal testing machine (QLW-5E, Qunlong, China), where an electrochemical workstation (Chenhua, CHI660E, China) was used to continuously record the corresponding electrical signal changes with strains. The participants for the real-life test for sensors were the authors (W. Q. She and Z. F. Xue) of this article, who performed with the full, informed consent provided informed consent. Ethical approval was not required for this work.

Statistical Analysis: Statistical evaluations were conducted using Origin (USA) and SPSS statistics software (IBM 26, USA). Data were presented as means \pm standard deviations (SD) from at least three independent experiments. Unpaired Student's t-test (two-tailed) assessed the significance of differences, with significance considered at $p < 0.05$ (* $p < 0.05$, ** $p < 0.01$, *** $p < 0.001$).

Figures

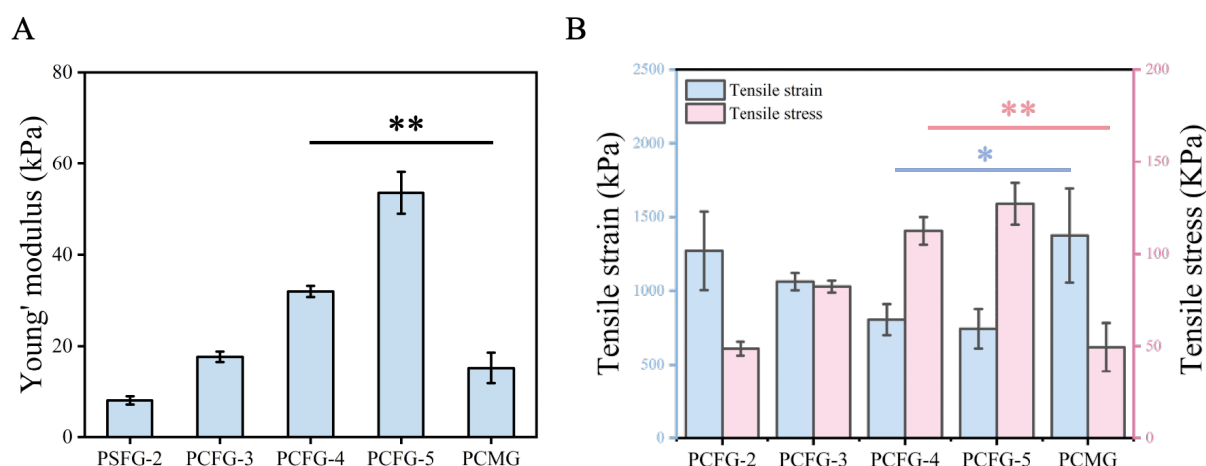


Figure S1. Mechanical properties of hydrogels. A) Young's modulus of hydrogels. B) Tensile strength and strain of hydrogels.

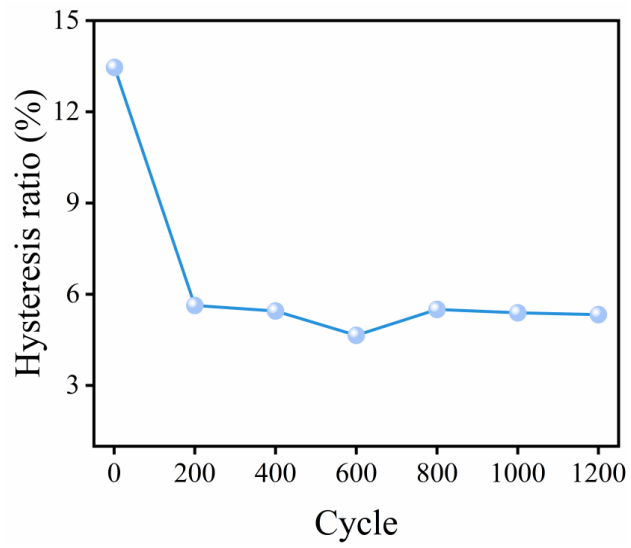
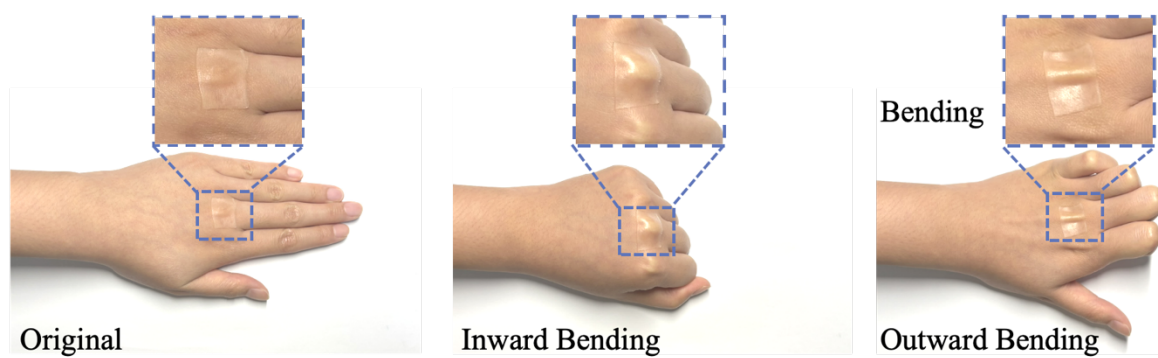


Figure S2. Hysteresis ratios of the PCFG-4 hydrogel at different cycles.

A



B

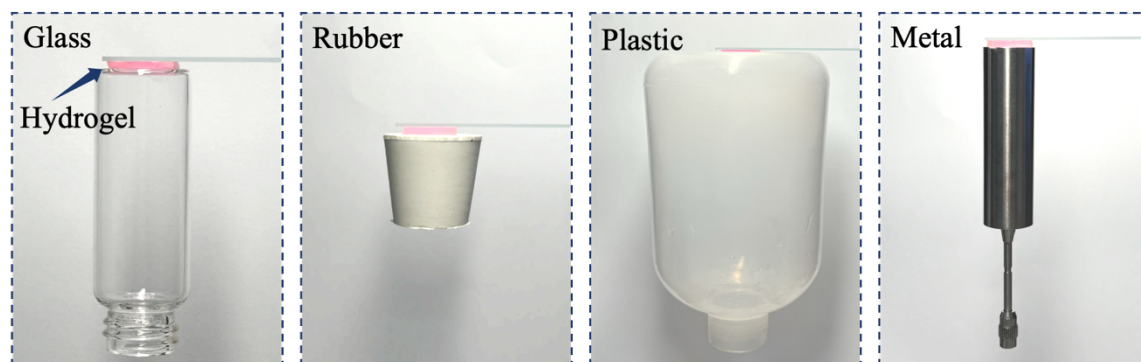


Figure S3. Photographs of the PCFG-4 hydrogel adhered to complex human skin (A) and various material surfaces (B).

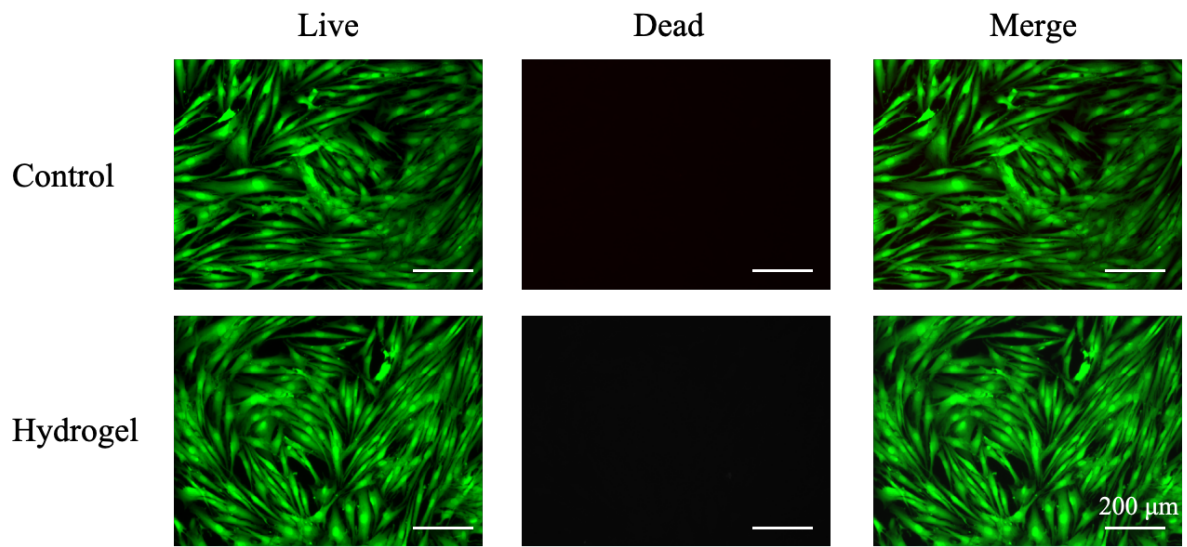
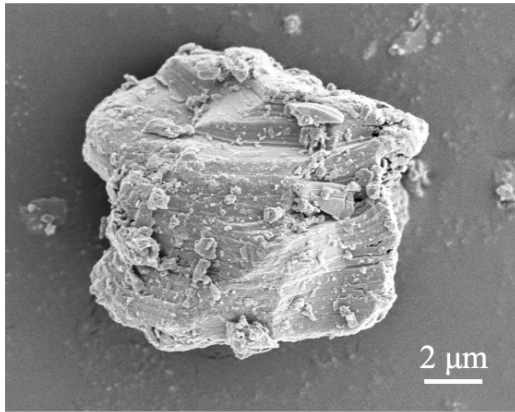
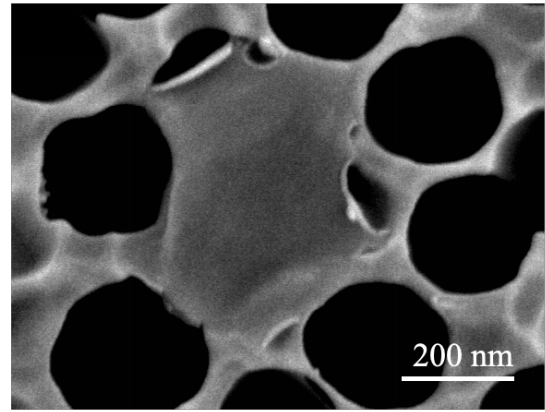


Figure S4. Live/dead staining of Fibroblast (HF) cells cultured for 24 h in hydrogel extracts.

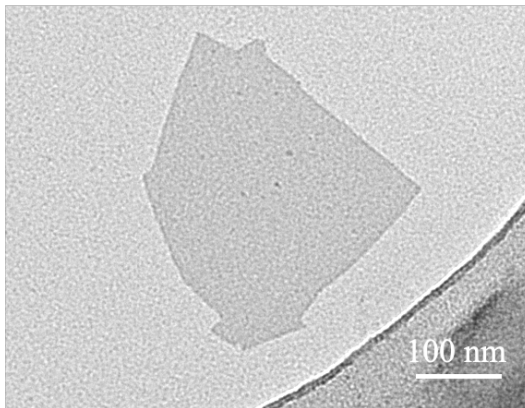
A



B



C



D

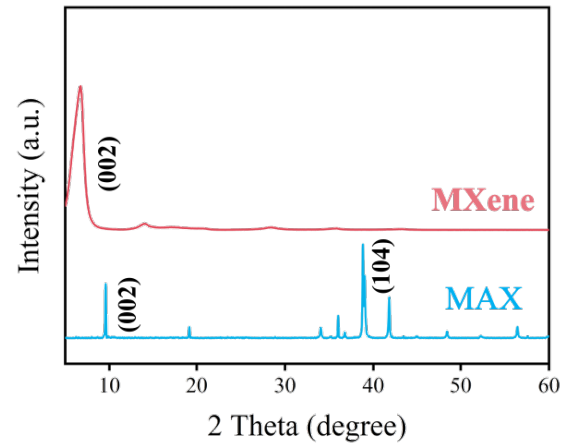


Figure S5. Characterization of MXene. A-B) SEM images of MAX phase (A) and MXene (B). C) Transmission Electron Microscope (TEM) image of MXene. D) X-ray diffraction (XRD) patterns of MAX phase and MXene.

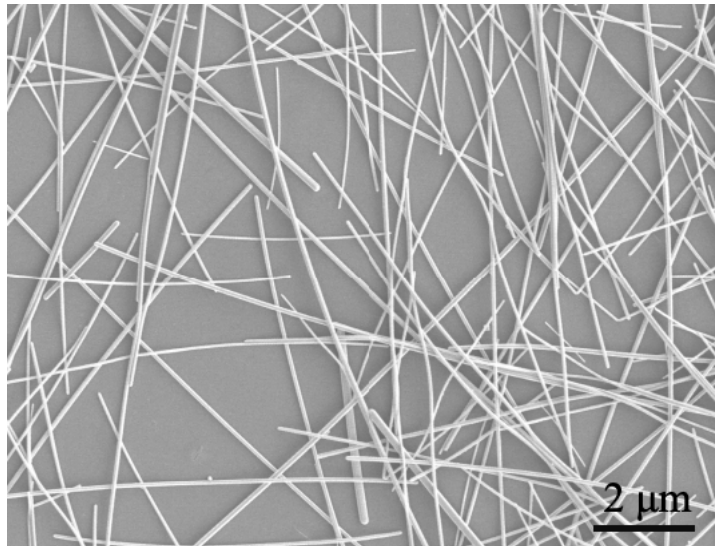
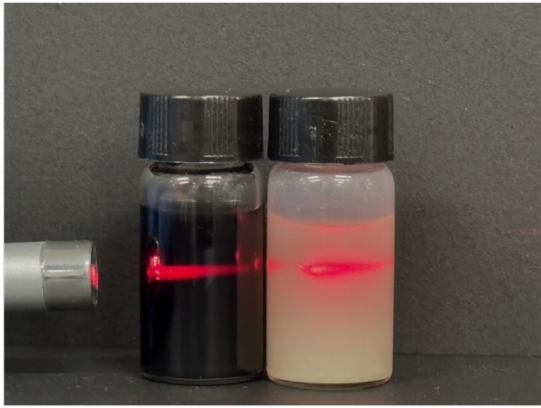


Figure S6. Morphological characteristics of AgNWs.

A



B



Figure S7. A) Tyndall effect of MXene and AgNW inks. B) Flocculation of the AgNW and MXene.

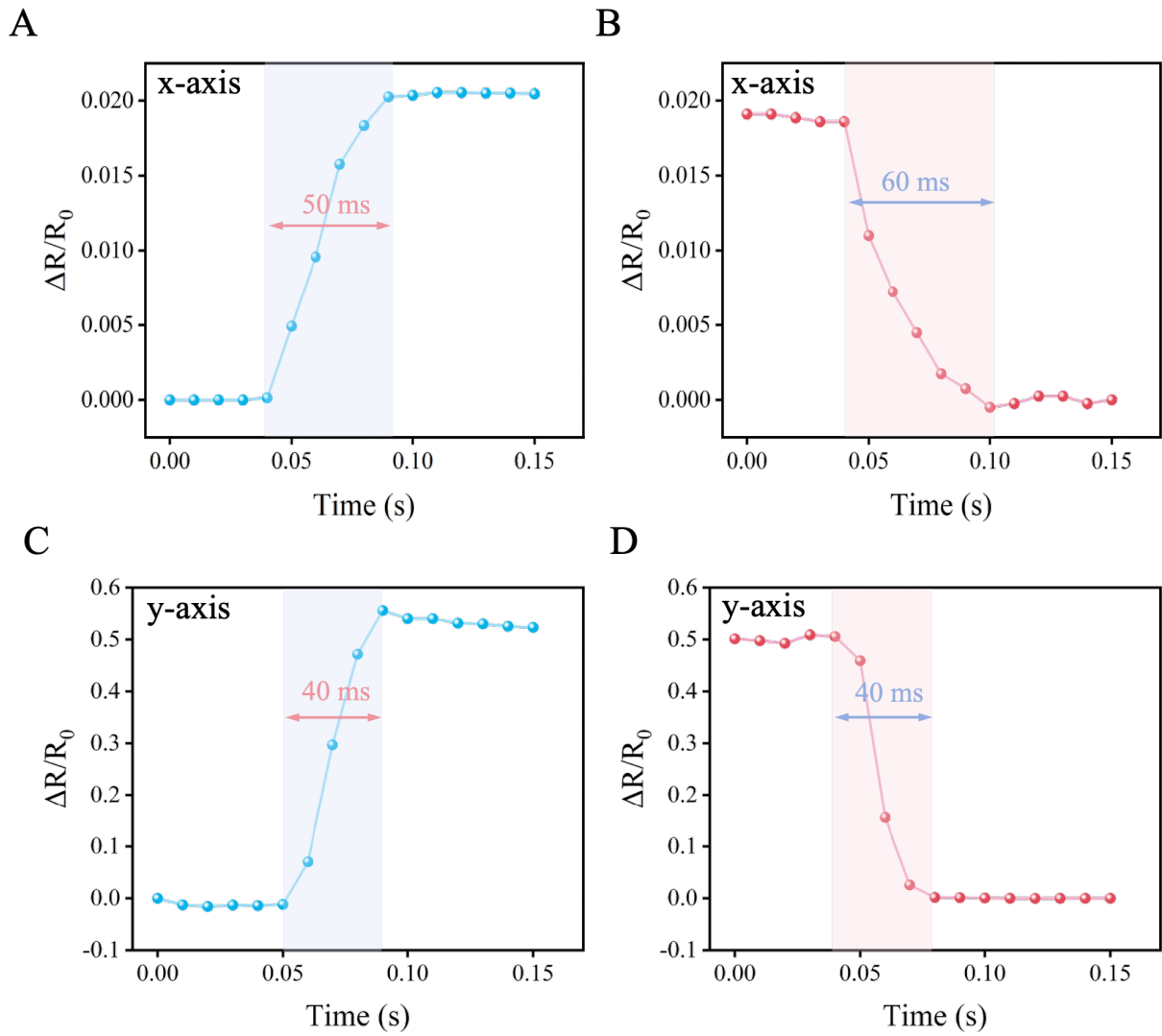


Figure S8. Response and recovery time of the AM-PCFG-4 sensor. A-B) Response (A) and recovery (B) time of the AM-PCFG-4 sensor in the x-axis direction. C-D) Response (C) and recovery (D) time of the AM-PCFG-4 sensor in the y-axis direction.

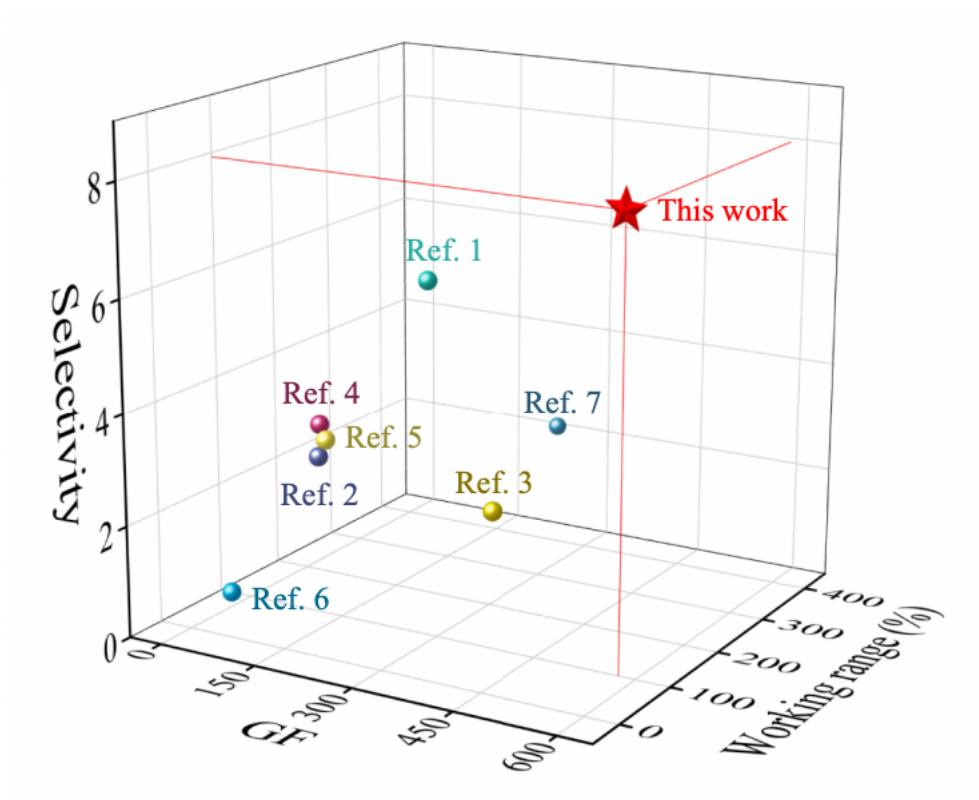


Figure S9. Comparison of selectivity, GF, and working range with recently reported multidirectional strain sensors in non-hydrogel systems.¹⁻⁷

References:

1. H. Zhang, D. Liu, J. H. Lee, H. M. Chen, E. Kim, X. Shen, Q. B. Zheng, J. L. Yang and K. Y. Kim, *Nano-Micro Lett*, 2021, **13**, 122.
2. J. H. Lee, J. Kim, D. Liu, F. M. Guo, X. Shen, Q. B. Zheng, S. Jeon and J. K. Kim, *Adv Funct Mater*, 2019, **29**, 1901623.
3. Y. F. Hu, T. Q. Huang, H. J. Lin, L. W. Ke, W. Cao, C. Chen, W. Q. Wang, K. Rui and J. X. Zhu, *J Mater Chem A*, 2022, **10**, 928-938.
4. Y. J. Liu, Z. Y. Wang, X. Y. Song, X. Shen, Y. Wei, C. X. Hua, P. P. Shao, D. P. Qu, J. Jiang and Y. Liu, *Small*, 2024, **20**, 2404810.
5. H. M. Chen, Y. Jing, J. H. Lee, D. Liu, J. Kim, S. S. Chen, K. Huang, X. Shen, Q. B. Zheng, J. L. Yang, S. Jeon and J. K. Kim, *Materials Horizons*, 2020, **7**, 2378-2389.
6. L. Zhao, J. Qiao, F. Li, D. Yuan, J. Huang, M. Wang and S. Xu, *ACS Appl Mater Interfaces*, 2022, **14**, 48276-48284.
7. G. Yang, X. Tang, G. Zhao, Y. Li, C. Ma, X. Zhuang and J. Yan, *Chem Eng J*, 2022, **435**, 135004.